NON-EQUILIBRIUM DYNAMICS AND COLLECTIVITY IN ULTRA-RELATIVISTIC PROTON–NUCLEUS COLLISIONS*

Lucia Oliva[a,b,c], Wenkai Fan[d], Pierre Moreau[d]
Steffen A. Bass[d], Elena Bratkovskaya[c,e,f]

[a]Department of Physics and Astronomy "Ettore Majorana", University of Catania
Via S. Sofia 64, 95123 Catania, Italy
[b]INFN Sezione di Catania, Via S. Sofia 64, 95123 Catania, Italy
[c]Institute for Theoretical Physics, Johann Wolfgang Goethe Universität
60438 Frankfurt am Main, Germany
[d]Department of Physics, Duke University, Durham, NC 27708, USA
[e]GSI Helmholtzzentrum für Schwerionenforschung GmbH
Planckstrasse 1, 64291 Darmstadt, Germany
[f]Helmholtz Research Academy Hesse for FAIR (HFHF)
GSI Helmholtz Center for Heavy Ion Physics
Campus Frankfurt, 60438 Frankfurt, Germany

Received 31 July 2022, accepted 22 August 2022,
published online 14 December 2022

We investigate the medium evolution in p+Pb collisions at LHC energy by comparing a non-equilibrium transport approach, PHSD, with a (2+1)D viscous hydrodynamic model, VISHNew, with initial conditions extracted from PHSD. We find that the energy density in PHSD is highly inhomogeneous in the transverse plane during the whole evolution, whereas VISHNew dissolves efficiently the initial spatial irregularities. We perform also a comparison of event topology in the two approaches by means of the transverse spherocity observable. We found that the spherocity distribution in PHSD is slightly shifted towards the isotropic limit with respect to the hydrodynamic case, mainly due to the different descriptions within the two models of the medium produced in small systems. We have applied the spherocity selection to the elliptic flow of charged particles finding that it is predominantly determined by the most jetty events. This finding supports the idea that multi-differential measurements through multiplicity and spherocity are very useful to study final-state observables in ultra-relativistic proton–nucleus collisions.

DOI:10.5506/APhysPolBSupp.16.1-A68

* Presented at the 29[th] International Conference on Ultrarelativistic Nucleus–Nucleus Collisions: Quark Matter 2022, Kraków, Poland, 4–10 April, 2022.

1. Introduction

There is an increasing interest in classifying events according not only to multiplicity but also to event topology. Transverse spherocity is an observable able to distinguish events according to their geometrical shape. Recent experimental results demonstrate the usefulness of a transverse spherocity analysis in small systems for studies related to collective flows and strangeness enhancement [1], which are considered as signatures for the formation of the Quark–Gluon Plasma (QGP), previously attributed only to heavy-ion collisions. We investigate the medium evolution and the transverse spherocity distribution in p+Pb collisions at LHC energy by comparing a non-equilibrium transport approach [2–4] with a viscous hydrodynamic model [5, 6]. We perform also a preliminary study on charged-particle elliptic flow applying the transverse spherocity analysis.

2. Model description and initialization

Model I: the Parton–Hadron-String Dynamics (PHSD) approach

PHSD is a covariant dynamical model for strongly interacting many-body systems based on generalized transport equations which are derived from the off-shell Kadanoff–Baym equations for non-equilibrium Green functions and fully describe the time evolution of both partonic and hadronic phases [2, 3]. PHSD simulates the full space-time evolution of the collision since the primary nucleon–nucleon inelastic scatterings between the two impinging nuclei, through QGP formation — when the local energy density is above the deconfinement transition value — to the hadronization and evolution in the hadronic phase. The Dynamical Quasi-Particle Model (DQPM) [3] describes the properties of the QGP in terms of parton spectral functions whose parameters are determined through the lattice QCD Equation of State (EoS). The shear and bulk viscosities of the QGP, determined from the partonic interaction rates in the DQPM, result in line with lattice QCD calculations [7, 8]. A dynamical hadronization process describes the fusion of off-shell quarks and antiquarks to off-shell hadronic states [3, 4].

Model II: hydrodynamic approach + hadronic afterburner

This hybrid approach [5] simulates the hot and dense QGP phase of the nuclear collision using the boost-invariant relativistic viscous hydrodynamics model in 2+1 dimensions VISHNew [6] and the cooler and more dilute regions of the fireball employing the relativistic Boltzmann transport model Ultrarelativistic Quantum Molecular Dynamics (UrQMD) [9, 10]. In VISHNew, the QGP space-time evolution is determined by means of the conservation equations $\partial_\mu T^{\mu\nu} = 0$ for the energy-momentum tensor of the viscous fluid. In order to solve them, the initial conditions for the fluid flow velocity u^{μ}, the energy density e, and equilibrium pressure P in the fluid rest frame, the bulk viscous pressure Π, and the shear stress tensor $\pi^{\mu\nu}$ should be provided at the thermalization time t_0 of the medium. We extract those initial conditions from PHSD by means of a Landau matching procedure; see Refs. [11, 12] for details. The time evolution of the viscous corrections is calculated through the second-order Israel–Stewart equations in the 14-momentum approximation [13]. The hydrodynamic simulations use the same $\eta/s(T)$ of PHSD and a parametrization for the bulk viscosity that resembles the PHSD one [11]. The hydrodynamic equations of motion are closed by an EoS based on lattice QCD calculations and then blended into a hadron resonance gas EoS [5]. This EoS is compatible with the one reproduced by the DQPM in PHSD. Below a switching temperature, the hydrodynamic medium is converted into particles through a Cooper–Frye algorithm and the hadronic matter is evolved microscopically with UrQMD.

For details on the two models, see Ref. [12].

3. Medium evolution: VISHNew versus PHSD

We compare the microscopic PHSD evolution with the macroscopic hydrodynamic evolution in VISHNew, with initial condition extracted from PHSD events in order to reduce the impact of the early out-of-equilibrium dynamics. Even though the two models share the same initial condition at

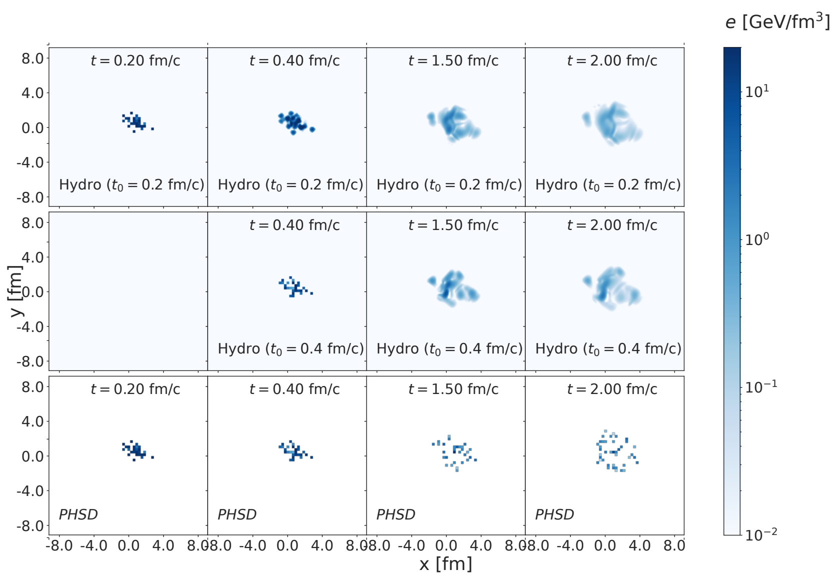

Fig. 1. Time evolution of the local energy density e in the transverse plane at $z = 0$ of a single event in PHSD and VISHNew for p+Pb collisions at $\sqrt{s_{NN}} = 5.02$ TeV with $b = 2$ fm; results for two different initial times t_0 in VISHNew are shown.

t_0, the subsequent evolution is different due to the different underlying dynamics. From Fig. 1 we see that the energy density decreases rapidly as the medium expands. The energy density profile in PHSD is highly inhomogeneous in the transverse plane during the full time evolution. In VISHNew, the energy density profile (after t_0) becomes smoother since the hot spots dissolve more efficiently with respect to PHSD, but still keeps a high level of inhomogeneity due to the small size of the medium produced in p+Pb collisions. The evolution of the energy density in the VISHNew results depends on the initialization time: the simulation with $t_0 = 0.4$ fm/c retains more hot spots than that starting at 0.2 fm/c because the medium is already more diluted and the time to smooth the spikes coming from the initial conditions is shorter before the system reaches the switching temperature.

4. Transverse spherocity and collectivity

The transverse spherocity (hereafter simply spherocity) S_0 is defined as

$$S_0 \equiv \frac{\pi^2}{4} \min_{\hat{\boldsymbol{n}}_{\boldsymbol{s}}} \left(\frac{\sum_i |\boldsymbol{p}_{\mathbf{T}\boldsymbol{i}} \times \hat{\boldsymbol{n}}_{\boldsymbol{s}}|}{\sum_i p_{\mathrm{T}i}} \right)^2 , \tag{1}$$

where $\hat{\boldsymbol{n}}_{\boldsymbol{s}}$ is a unit vector that minimizes the ratio in parenthesis, the sum runs over all charged particles in the pseudorapidity region $|\eta| < 0.5$ and transverse momentum p_{T} within a given interval. The limit $S_0 \to 0$ corresponds to "jetty" events, where all p_{T} vectors are (anti)parallel or their sum is dominated by a single track; the limit $S_0 \to 1$ indicates "isotropic" events, where the p_{T} vectors are isotropically distributed.

In Fig. 2 we present the event probability P as a function of the number of charged particle N_{ch} (a) and the spherocity S_0 (b). The gray (orange) lines are the PHSD results, while the black (blue) curves are obtained with the hydrodynamic simulations. In panel (a), we see that $P(N_{\mathrm{ch}})$ is different in the two models, being shifted to higher values in the PHSD case. Moreover, by comparing the solid and dashed lines, we notice that in both approaches the event distribution is different when different p_{T} cuts are applied in the computation of N_{ch}. From panel (b) we see that the spherocity distribution in PHSD is shifted more towards 1 compared to hydrodynamics and is similar to predictions from other transport models [14]. Even though $P(N_{\mathrm{ch}})$ is substantially modified in both hydrodynamics and PHSD when different p_{T} cuts are applied, $P(S_0)$ does not change visibly within the same approach. This indicates that the dissimilarity between PHSD and hydrodynamics in the $P(S_0)$ is not strongly related to the difference in the N_{ch} distribution but is rather due to the different descriptions within the two models of the medium produced in small colliding systems since the event topology is mainly decided by the underlying particle production dynamics and medium effects [15].

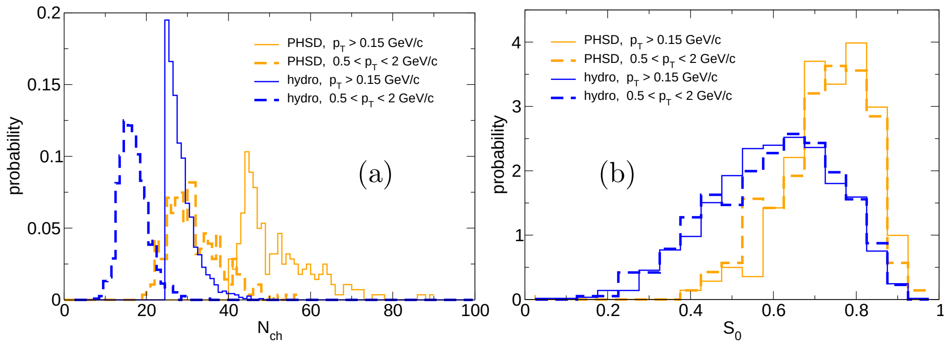

Fig. 2. (Color on-line) Event distribution as a function of charged particles (a) and spherocity (b) at midrapidity $|\eta| < 0.5$ for PHSD (gray/orange lines) and hydrodynamics (black/blue lines) considering different $p_{\rm T}$ ranges. The initial conditions for VISHNew are extracted at $t_0 = 0.4$ fm/c from minimum bias PHSD collisions and then the 5% most central events are selected within each of the two approaches.

As a first preliminary application of the multi-differential method, we show in Fig. 3 the PHSD results for the $p_{\rm T}$ dependence of charged-particle elliptic flow v_2 in the 0–10% centrality class. The v_2 in small systems has been investigated with PHSD in Ref. [16], but here we present the results with the spherocity selection. In Fig. 3, the solid (red) line corresponds to the v_2 without selection in spherocity, while the dash-dotted (blue) and dashed (green) lines are obtained selecting the 20% events with, respectively, higher and lower S_0. We clearly see that isotropic events have a $v_2 \approx 0$, whereas the jetty events present the predominant contribution to the v_2 of spherocity-integrated events, in agreement with AMPT results for Pb+Pb collisions [14]. We notice that there is a non-trivial relation between event classifiers, such as multiplicity and spherocity, in small systems. In-

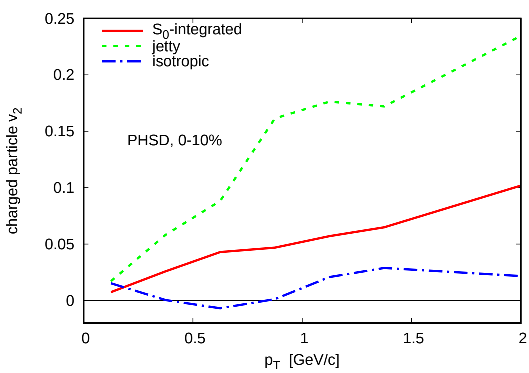

Fig. 3. (Color on-line) Elliptic flow of charged particles as a function of transverse momentum at midrapidity for 10% central p+Pb collisions at $\sqrt{s_{NN}} = 5.02$ TeV.

deed, it has been shown that in both Pb+Pb and p+p collisions more central events, *i.e.* with higher multiplicity, correspond to more isotropic topologies and events with lower multiplicity are more jetty [15]. In heavy-ion collisions, the v_2 is higher in semi-peripheral collisions, while more central events have a small v_2, therefore,there is a correspondence between multiplicity and spherocity when looking at the magnitude of the v_2. This is not the case for proton–nucleus collisions since the v_2 is higher in jetty events (see Fig. 3) but we expect a higher v_2 in high-multiplicity events (corresponding to more isotropic configurations). This highlights the importance to perform a multi-differential event classification according to both $N_{\rm ch}$ and S_0 when studying the elliptic flow v_2 in small systems.

L.O. and E.B. acknowledge support by the Deutsche Forschungsgemeinschaft (DFG) through the grant CRC-TR 211 “Strong-interaction matter under extreme conditions” No. 315477589–TRR 211. L.O. has been in part financially funded by the Alexander von Humboldt-Stiftung. W.F., P.M., and S.A.B. has been supported by the U.S. Department of Energy Grant No. DE-FG02-05ER41367. The computational resources have been provided by the Goethe-HLR Center for Scientific Computing.

REFERENCES

[1] A. Nassirpour, *J. Phys.: Conf. Ser.* **1602**, 012007 (2020).
[2] W. Cassing, E.L. Bratkovskaya, *Phys. Rev. C* **78**, 034919 (2008).
[3] W. Cassing, E.L. Bratkovskaya, *Nucl. Phys. A* **831**, 215 (2009).
[4] E.L. Bratkovskaya, W. Cassing, V.P. Konchakovski, O. Linnyk, *Nucl. Phys. A* **856**, 162 (2011).
[5] J.S. Moreland, J.E. Bernhard, S.A. Bass, *Phys. Rev. C* **101**, 024911 (2020).
[6] C. Shen *et al.*, *Comput. Phys. Commun.* **199**, 61 (2016).
[7] O. Soloveva, P. Moreau, E. Bratkovskaya, *Phys. Rev. C* **101**, 045203 (2020).
[8] P. Moreau *et al.*, *Phys. Rev. C* **100**, 014911 (2019).
[9] S.A. Bass *et al.*, *Prog. Part. Nucl. Phys.* **41**, 255 (1998).
[10] M. Bleicher *et al.*, *J. Phys. G: Nucl. Part. Phys.* **25**, 1859 (1999).
[11] Y. Xu *et al.*, *Phys. Rev. C* **96**, 024902 (2017).
[12] L. Oliva *et al.*, `arXiv:2204.04194 [nucl-th]`.
[13] G.S. Denicol, S. Jeon, C. Gale, *Phys. Rev. C* **90**, 024912 (2014).
[14] N. Mallick, R. Sahoo, S. Tripathy, A. Ortiz, *J. Phys. G: Nucl. Part. Phys.* **48**, 045104 (2021).
[15] S. Prasad *et al.*, *Sci. Rep.* **12**, 3917 (2022).
[16] L. Oliva, P. Moreau, V. Voronyuk, E. Bratkovskaya, *Phys. Rev. C* **101**, 014917 (2020).